International Conference on Computational Methods in Marine Engineering
MARINE 2011
L.Eça, E. Oñate, J. García, T. Kvamsdal and P. Bergan (Eds)

STRUCTURAL PERFORMANCE AND DYNAMIC RESPONSE OF SEMI-SUBMERSIBLE OFFSHORE PLATFORMS USING A FULLY COUPLED FE-SPH APPROACH

MARINE 2011

PAUL J. CROAKER[†], FOUAD EL-KHALDI[‡], PAUL H. L. GROENENBOOM[*], BRUCE K. CARTWRIGHT[†] AND ARGIRIS KAMOULAKOS[‡]

[†] Pacific Engineering Systems International Pty Ltd
277-279 Broadway, Broadway NSW 2007, Australia
e-mail: paulc@esi.com.au, brucec@esi.com.au

[‡] ESI Group
Parc d'Affaires SILIC, 99 rue des Solets, BP 80112, 94513 Rungis CEDEX, France
Email: Fouad.el.Khaldi@esi-group.com, Argiris.Kamoulakos@esi-group.com

[*] ESI Group Netherlands
Rotterdamseweg 183 C, 2629 HD Delft, The Netherlands
e-mail: Paul.Groenenboom@esi-group.com - Web page: http://www.esi-group.com

Key words: Smoothed Particle Hydrodynamics, Dynamic Stability, Offshore Platforms.

Summary. An explicit Finite Element (FE) software package with an embedded and fully coupled Smoothed Particle Hydrodynamics (SPH) solver is used to investigate the dynamic response of a floating (moored) offshore platform subject to strong wave action. The water is modelled using SPH while the platform and anchor cables are modelled using FE. The main body of the platform is modelled as a rigid body with appropriate mass, centre of gravity and moments of inertia. Coupling between the SPH and FE is automatically handled by contact algorithms available in the solver[1]. To represent the effect of the mooring system on the dynamic response of the platform, the anchor cables are modelled using flexible 1-dimensional (1D) finite elements. The stable time step for these 1D elements is much smaller than for the SPH particles and including the flexible anchor cables in the model would ordinarily cause excessive simulation times. However, a technique known as multi-model coupling is used to partition the analysis model into 2 separate models, each of which advances at its own stable time step[2]. This technique is shown to result in a total simulation time that is comparable to that obtained when running the case without anchor cables. The use of periodic boundary conditions applied to the SPH particles allowed the computational domain to be limited to 4 wavelengths in the direction of wave travel. The waves are generated by applying the moving floor technique[3]. The dynamic response of the platform is presented for the case when the platform is operating at a depth of 310 m under the influence of waves with a wavelength of 365 m and amplitude of 7.8 m. This represents the survival condition for a reference semi-submersible platform. An extension of this approach considering the stresses induced in structural members of the platforms is also demonstrated by replacing the rigid representation of the cranes with flexible finite elements.

1 INTRODUCTION

An offshore platform such as a Semi-Submersible or FPSO (Floating Platform Storage and Offloading) used in the oil and gas industry has to operate in a hostile environment. With increasing demand for these resources, such structures are being placed in deeper and deeper waters and further out to sea, and hence have to survive increasingly severe conditions. As these structures are commonly moored at one location for up to 20 years, they need to be designed to withstand the direct and the indirect effect of the ocean waves over an extended period of time. The waves will by necessity include regular waves of the prevailing geographical location, irregular, large amplitude, breaking waves associated with isolated storms, and possibly rogue waves that may occur in water of any depth[4]. Waves directly impact on a platform's critical structural features and can produce cumulative and occasionally isolated damage which can trigger catastrophic failure of the structure. Similarly, large waves may also result in green water on the deck, and although damage may not be structurally catastrophic, there may be a significant loss of production capability due to inoperable process equipment, uninhabitable living quarters, and/or injured personnel.

In an era where reliable virtual prototyping is 'de rigueur' in many fields, engineers need to be able to model the underlying physics of such scenarios sufficiently well that structures can survive and operate effectively in these harsh and demanding environments.

The older approach to the computational assessment of hydrodynamic loads on these offshore platforms, or floating objects in general, is based predominantly on the numerical solution of a set of equations for fluid flow within a continuous domain. It usually includes simplifying assumptions such as the flow being irrotational, or the solution being based on diffraction theory. Such solution methods have limitations with respect to the shape of the free surface and often rely heavily on empirical formulae. For reasonably smooth waves and/or simple hull shapes, such solutions may be adequate. Unfortunately, for the common phenomena of breaking waves and green water, or the extreme case of a rogue wave, the validity of such assumptions no longer applies. Although these traditional design tools will still produce a solution, it is unreliable.

Contemporary offshore designs such as semi-submersible platforms venture further from the empirical base on which the traditional tools were developed, further jeopardising the reliability of the solution. The currently available empirical tools typically do not allow the accurate consideration of physical scenarios such as slamming or violent wave impact, where the effect of the entrapped air or local rough water may be relevant.

More recent approaches, independent of any empirical relationships and simplifying assumptions, decouple the fluid-flow and structural problems. Typically, a hydrodynamic analysis is used to obtain pressures at various hull locations, and these pressures are subsequently transferred to a finite element code for structural analysis in order to assess the integrity of the platform structure. The hydrodynamic analysis may use a conventional computational fluid dynamics (CFD) code prior to the structural analysis by a conventional, stand-alone, FE code[5]. Alternatively, that hydrodynamic analysis may be done using a code based on a meshless technique such as the smoothed particle hydrodynamics (SPH) method[6,7].

Although this decoupled approach represents a significant improvement over the empirical methods for novel geometry and severe wave scenarios, it still has several flaws. The major

one of these is that for severe dynamic loads, the loads themselves will be influenced by the displacements of the structure i.e. the concept of hydro-elasticity.

The technique employed in this paper is a fully coupled solution, where the fluid and the structural response are solved simultaneously and continuously throughout both the spatial domain and the duration of the simulation, thus enabling a true hydro-elastic solution. The technique utilises a hybridised solver that incorporates a mesh-free particle solver for the fluid domain and a non-linear finite element solver in the one code. This hybridised solver has previously demonstrated the capability to handle rigid structures in severe waves[8,9] and is extended here to include flexible components of the structure.

2 NUMERICAL METHODS

2.1 Overview

The commercial finite element code Virtual Performance Solution (PAM-CRASH), or VPS[2,] produces the numerical results presented here. With a long pedigree of use in the automotive and aerospace sectors, this is a general purpose code with an explicit solver optimised for dynamic, strongly non-linear structural mechanics, and contains finite element formulations for thin shells, solid elements, membranes and beams with material models with plasticity and failure for metals, plastics, rubbers, foams and composites. A Smoothed Particle Hydrodynamics (SPH) solver integrated within the explicit solver enables both finite elements and SPH elements to be used and solved simultaneously in the same model.

The SPH method is an interpolation method in which each "particle" describes a fixed amount of material in a Lagrangian reference frame. As the method needs no mesh, SPH can handle the motion and topology changes of material surfaces simply. The evaluation of field variables such as density and velocity at the location of a selected particle is done by interpolation over all neighbour particles in a region of influence as shown in Figure 1.

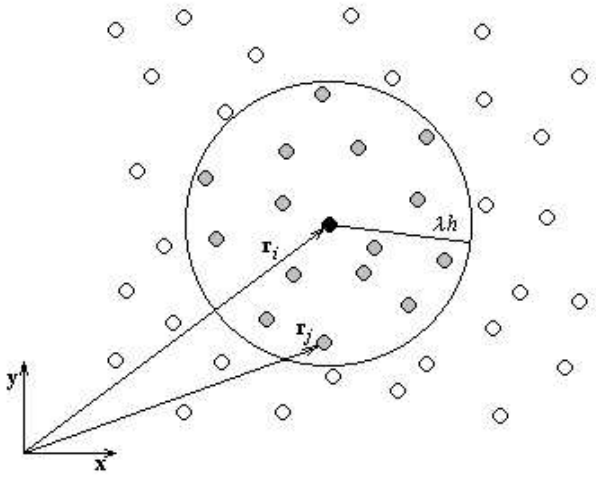

Figure 1 : Two-dimensional representation of the region of influence of particle 'i'.

The size of the sphere (or circle in 2D) of this region, is defined by the smoothing length h. An important advantage of the SPH method is that spatial derivatives of the unknown field

variables may be evaluated using the known derivative of the smoothing kernel. Unless mentioned otherwise, the method discussed here is basically similar to that of Monaghan[10,11]. In the equations below, the undefined symbols have their customary meaning.

Within the SPH method, the derivative of the density for particle 'i' may be solved from the continuity equation (1):

$$\frac{\mathrm{d}\rho_i}{\mathrm{d}t} = \sum_j m_j (\mathrm{v}_i - \mathrm{v}_j) \cdot \nabla_i W_{ij} \tag{1}$$

where the sum extends over all neighbour particles and W is the smoothing kernel evaluated at the distance between particles i and j. Optionally, renormalisation of the density field may be performed[12]. The updated velocity may be obtained from the momentum equation (2):

$$\frac{\mathrm{d}\mathrm{v}_i}{\mathrm{d}t} = -\sum_j m_j \left(\frac{p_i}{\rho_i^2} + \frac{p}{\rho_j^2} + \Pi_{ij}\right) \cdot \nabla_i W_{ij} \tag{2}$$

in which artificial viscosity is defined by equation (3):

$$\Pi_{ij} = \frac{2}{\rho_i + \rho_j} \left(-\alpha \frac{c_i + c_j}{2} \mu_{ij} + \beta \mu_{ij}^2 \right) \tag{3}$$

where

$$\mu_{ij} = \begin{cases} \frac{1}{2}(h_i + h_j) \dfrac{(\mathrm{v}_i - \mathrm{v}_j) \cdot (\mathrm{r}_i - \mathrm{r}_j)}{|\mathrm{r}_i - \mathrm{r}_j|^2 + \eta^2}, & (\mathrm{v}_i - \mathrm{v}_j) \cdot (\mathrm{r}_i - \mathrm{r}_j) < 0 \\ 0, & (\mathrm{v}_i - \mathrm{v}_j) \cdot (\mathrm{r}_i - \mathrm{r}_j) \geq 0 \end{cases} \tag{4}$$

The values of α and β determine the strength of the artificial viscosity required to suppress numerical shocks. Values (as low as possible) should be used to prevent the flow becoming too viscous. In equation (4), η is a corrective constant avoiding creation of a singularity when particles approach each other. Regular particle positions are achieved when the anti-crossing option (XSPH)[10] is employed, as expressed in equation (5):

$$\frac{\mathrm{d}\mathrm{r}_i}{\mathrm{d}t} = \mathrm{v}_i + \varepsilon \sum_j m_j \frac{(\mathrm{v}_i - \mathrm{v}_j)}{\frac{1}{2}(\rho_i + \rho_j)} W_{ij} \tag{5}$$

For a non-zero ε parameter, equation (5) is used to update the particle positions, whereas the strains remain based on the uncorrected displacements. The cubic spline kernel, given by equation (6), is used for the smoothing kernel.

$$W(|\mathrm{r} - \mathrm{r}'|, h) = \begin{cases} \frac{N}{h^D} \left[\frac{3}{4} \left(\frac{|\mathrm{r}-\mathrm{r}'|}{h} \right)^3 - \frac{3}{2} \left(\frac{|\mathrm{r}-\mathrm{r}'|}{h} \right)^2 + 1 \right], & 0 \leq \frac{|\mathrm{r}-\mathrm{r}'|}{h} < 1 \\ \frac{1}{4} \frac{N}{h^D} \left[2 - \left(\frac{|\mathrm{r}-\mathrm{r}'|}{h} \right) \right]^3, & 1 \leq \frac{|\mathrm{r}-\mathrm{r}'|}{h} < 2 \\ 0, & 2 \leq \frac{|\mathrm{r}-\mathrm{r}'|}{h} \end{cases} \tag{6}$$

In the preceding, the smoothing length, h, is proportional to the particle radius, N is a normalisation constant, and D is the dimension of the model[1,2,3].

The flow will be assumed to be nearly incompressible implying that the pressure field is obtained from an equation of state (EOS) model. Herein, the Murnaghan EOS, equation (7), is used for water, in which B is a bulk modulus of 2.2MPa, ρ is a density of 1,000 kg/m^3 and the exponent γ is taken as 7.

$$p = {}^0p + B\left[\left(\frac{\rho}{{}^0\rho}\right)^{\gamma} - 1\right] \tag{7}$$

Particles are assumed to interact mutually only if they are sufficiently close to each other; this being established by an efficient nearest neighbour (NN) search algorithm that does not need to be repeated each computational cycle. Second-order accurate leap-frog time stepping is used for the explicit time integration of the above rate equations. The numerical time step is set to a fraction (usually about 0.7) of the well-known CFL criterion based on the sound speed and smoothing length of all particles, or the size of the finite elements present in the model.

2.2 Contact Treatment

Robust contact algorithms in the code enable modelling of dynamic contact between various parts within a model. Interaction between particles representing a fluid and moving, or deformable, structures represented by finite elements may be modelled by one of the sliding interface contact algorithms available in VPS[2]. Such algorithms prevent the interpenetration of specified components while in most cases allowing sliding. These sliding interfaces are based on the well known penalty formulation, where geometrical interpenetrations between so-called slave nodes and adjacent master faces are penalized by counteracting forces that are essentially proportional to the penetration depth. The contact algorithm will automatically detect when a particle or node (slave) penetrates any segments (master) of the outer surface of the finite element model of the structure. The contact thickness indicates the distance away from a contact face where physical contact is established. For SPH particles as slaves, the contact thickness should be representative of the particle spacing. This type of contact has been validated by simulation of vertical motion of floating bodies. It has been found that the correct position is reached with accuracy even below the particle size when the thickness defined for the contact equals half the particle spacing and the artificial viscosity coefficients are taken significantly smaller than the values normally applied for shocks. In that case the upward force is also correct. The contact thickness and the relative strength of the repulsive forces may be defined in input. The use of the coupled FE-SPH algorithm has been used for a range of applications including sloshing[13], heart valve opening[14], bird strike and impact of aeronautical structures on water[15]. This contact will also be used to define rigid boundary conditions to limit the flow domain.

2.3 Periodic Boundary Conditions

For the numerical simulation of ships in waves using domain discretisation methods, a common approach is to limit the water domain by walls at sufficient distance from the hull and create waves by imposing appropriate displacement conditions on these walls. If the

motion of a travelling ship has to be followed for a relatively long period of time, the computational domain will have to be extended in the direction of travel which may lead to a large computational burden. When the vessel is travelling at a more or less constant speed in the same direction, an attractive alternative for the numerical simulation is to impose the average velocity to the water in the opposite direction. In that case it will be necessary to impose periodic boundary conditions in which water flowing out of the downstream section sufficiently far behind the stern will re-enter the domain at a section in front of the bow.

Periodic boundary conditions are available in many Eulerian CFD codes. It is also possible to implement periodic boundary conditions for SPH. Handling the kinematics is trivial when the surfaces are restricted to being flat and parallel. Since the dynamics of the SPH method demand the influence of the neighbouring particle in all directions be considered, there needs to be interaction between particles that have just been re-injected at the upstream boundary with particles that are sufficiently close to the downstream boundary. This has been accomplished by adding and subtracting the offset between the two corresponding periodic boundaries to the appropriate coordinate of all particles inside the domain, to determine the distance between any pair of particles when neighbours are being searched. The search algorithm has been extended to take the position of these virtual particles into account.

2.4 Multi-model Coupling

Multi-model coupling (MMC) is a unique feature integral to VPS[2] which allows two independent FE-SPH models to be efficiently joined and run as a single model[16]. This modelling technique unifies two FE-SPH models where the cycle time-step of one is much smaller than the other. By allocating different CPUs to each of the two models, and applying a mathematical technique called sub-cycling, each model is essentially run independently. Data is transferred between the two models by either a tied interface (which stipulates how the models are joined) or by a defined contact interface (which describes how they physically interact). This allows the two parts of the joined model to run at two different time-steps.

MMC allows the incorporation of detailed component models requiring a very fine time step without affecting the larger time-step of the global model. Herein, the global model consists of the main offshore platform structure, SPH particles representing the water, and detailed component models for the flexible anchor cables and crane structure.

3 MODEL DESCRIPTION

3.1 Offshore Platform Model

A finite element model of a generic semi-submersible offshore platform is created with dimensions and masses similar to operational platforms. The finite elements of the offshore platform are used to create a rigid body. This rigid body has the correct mass and inertia of the platform, and has a contact interface with the SPH particles representing the water. This approach allows the global motion of the platform under strong wave action to be investigated without the need to resolve the structural deformation of main structure of the platform. Such an approach significantly reduces the analysis times for these coupled FE-SPH analyses.

As the finite element model is an approximation of a generic semi-submersible offshore

platform, the hydrostatic equilibrium of the platform is unknown. In any analysis herein, the platform model is initially suspended above the water and allowed to drop under the influence of gravity, relying on the interaction with the SPH particles to reach its equilibrium position.

The inertias of the structure are estimated from an approximate distribution of structure and stores on the platform. The overall length and width of the platform are 105 m and 65 m respectively. The draft of the platform is 16.5 m with a displacement of 27.7 Mt. Figure 2 shows a diagram of the offshore platform model.

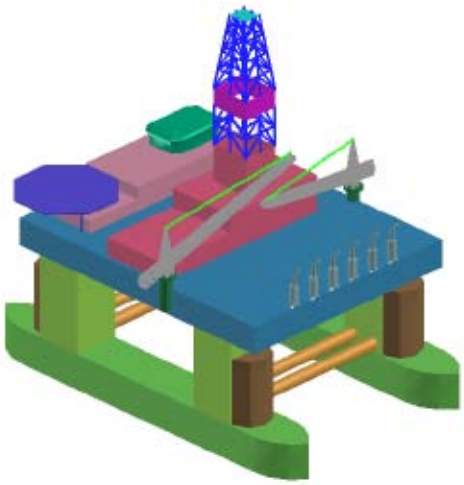

Figure 2 : Generic offshore platform model

3.2 Hydrodynamic Model

The offshore platform model is simulated with zero forward speed in regular head waves of 7.80m wave height and a wave length of 365m. The wave period is equal to approximately 15.2 seconds. While semi-submersible offshore platforms have engines that can be used for station keeping purposes, these engines have not been considered in the present work.

A computational domain of 1460m x 244m x 55m is used for the water. Approximately 2,400,000 SPH particles with a uniform spacing of 1m are used to fill the computational domain. Periodic boundary conditions are applied at the extents of the domain in the direction of wave travel to limit the size of the computational domain. The waves are generated by applying the moving floor technique of Cartwright et al[3].

3.3 Flexible Component Submodels

To investigate the structural deformation of certain components of the platform and assess their influence on the dynamic response of the platform, a separate model of these flexible components is created. This flexible component model is then connected to the rigid body of the main structure using the MMC technique[16]. All flexible components are steel, with a density of 7800 kg/m^3, elastic modulus of 210 GPa and Poisson's ratio of 0.3.

3.3.1 Flexible Mooring System

The primary aim of the present work is to investigate the effect of the mooring system on the dynamic response of the offshore platform. To achieve this aim, the anchor cables are represented by linear elastic 1D finite elements. The platform has 8 anchor cables. These are evenly distributed around the platform in a 'spread mooring' configuration. Each anchor cable is 1,000 m long and has a diameter of 0.09m.

A rigid plane is placed at a depth of 310m to represent the ocean floor. Each anchor cable extends from the platform to the ocean floor and then runs along the ocean floor. The ends of each cable are fixed in space by a displacement boundary condition. Contact is defined between the cables and the ocean floor.

3.3.2 Flexible Crane Structure

Also of interest in the present work are the structural deformations and stresses of vital on-board equipment. To this end, a model is created including crane structures as linear elastic, 1D, finite elements. The steel structural members of the crane are assumed to be pin-jointed together and made from constant cross-section tubular members with an outer and inner diameter of 0.10 and 0.09m respectively. Both the anchor cables and the crane structure are connected to the main offshore platform structure by tied interfaces.

4 RESULTS

As summarised in Table 1, three structural models are used for the analyses presented here. Figure 3 illustrates the computational domain of Analysis Model 3 showing the SPH (green), the ocean floor (purple) and the spread mooring cables (light grey). The waves that are generated by the moving floor (dark grey) travel from left to right.

Analysis Model	Main Platform Structure	Anchor Cables	Cranes
1	Rigid	Absent	Rigid
2	Rigid	Flexible	Rigid
3	Rigid	Flexible	Flexible

Table 1 : Summary of analysis models

4.1 Dynamic Stability of Platform

In operation, large anchors are attached to the end of the anchor cables. As the platform drifts downstream, tension in the anchor cable will exert a force on the anchor and this will result in the anchor being dragged along the ocean floor. This has not been included in the analyses considered here, with the anchor cables instead being fixed at their ends. As the platform drifts downstream, the two trailing anchor cables reach maximum extension after approximately 140 seconds. After this time, the stresses in the anchor cables rapidly exceed the ultimate tensile strength of the steel cables indicating that the anchor cables would fail. Failure of the anchor cables has not been considered in the present analyses and hence only results up to 160 seconds are presented here.

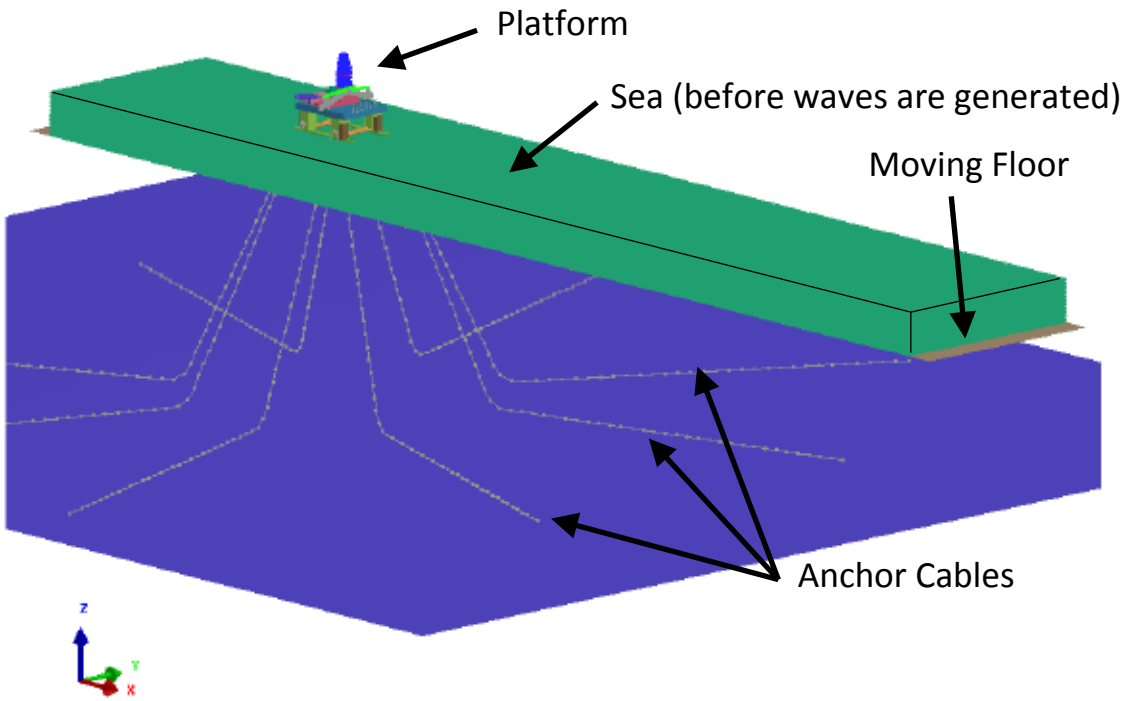

Figure 3: Analysis Model 3

The influence of the mooring system on the dynamic response of the platform under strong wave action is investigated by considering the global motion of the platform with, and without, anchor cables. Figure 4 shows the comparison of the surge, heave and pitch of the platform with, and without, anchor cables. In Figure 4, the solid line represents the platform without anchor cables, whereas the dashed line is used for the platform with anchor cables.

From Figure 4 it is clear that the platform with anchor cables undergoes greater pitching motion than the platform without. The forces applied to the structure by the anchor cables add an additional moment to the platform which induces larger rotations. Figure 4 also shows that the amplitude of the platform heave is larger for the platform with anchor cables. The heave motion shows that both platforms begin the analysis suspended above the water and are dropped into the water. Neutral buoyancy of the platforms is achieved after approximately 100 seconds. Figure 4 shows that the most marked difference in the dynamics of the platforms occurs for the surge motion. The platform with anchor cables experiences far greater surge than the platform without anchor cables. This may be due to the anchor cables causing a greater pitching motion of the platform, something that needs to be confirmed by further investigation. Such motion results in a larger component of the hydrostatic pressure force to be oriented in the direction of wave travel and it results in an increase in the platform surge.

Figure 5 shows the interaction of the platforms with the waves at three instances in time. The platform with, and without, anchor cables is shown on the right and left respectively.

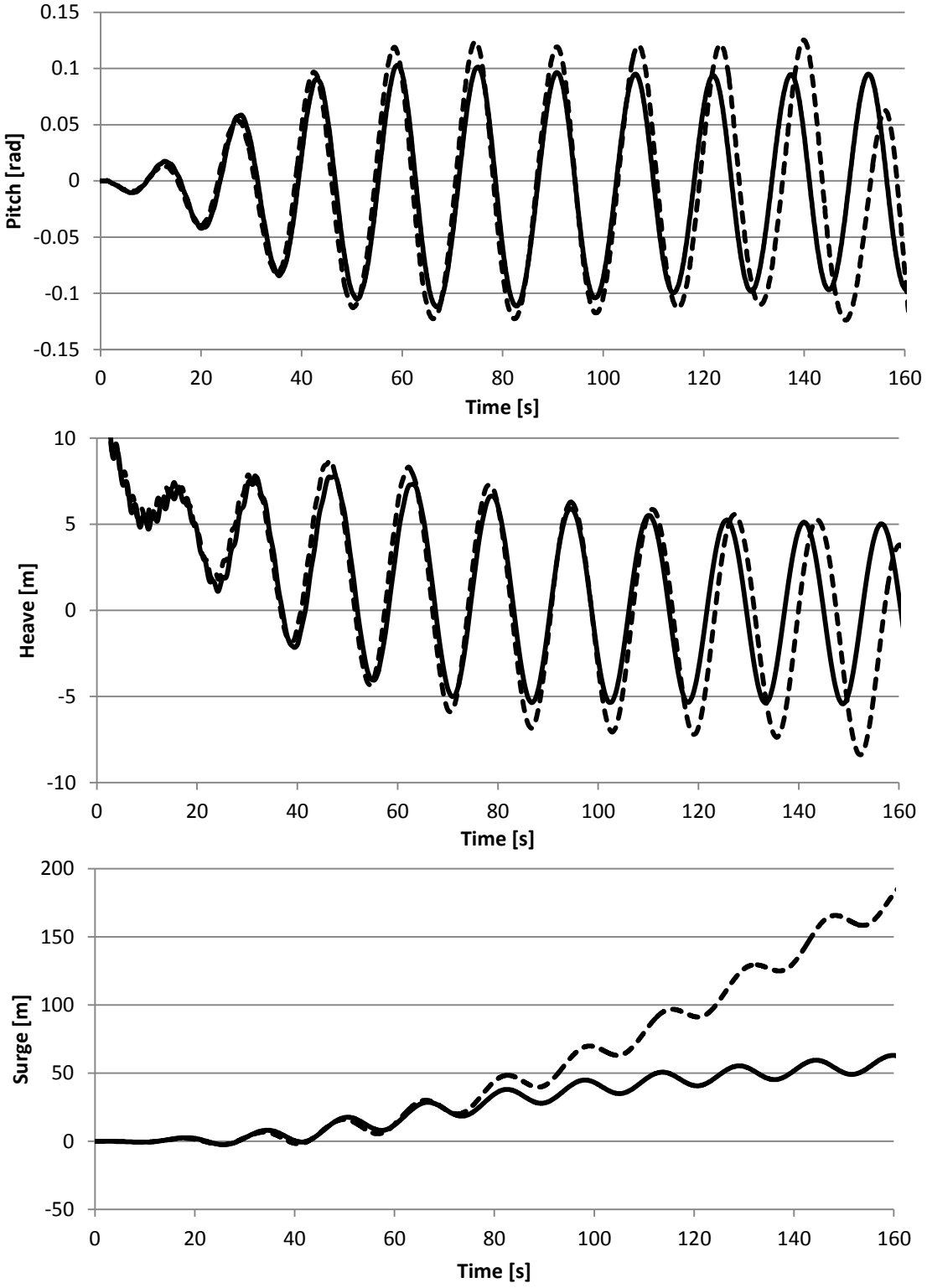
Pitch [rad]
0.15
0.1
0.05
0
-0.05
-0.1
-0.15
0
20
40
60
80
100
120
140
160
Time [s]
Heave [m]
10
5
0
-5
-10
0
20
40
60
80
100
120
140
160
Time [s]
Surge [m]
200
150
100
50
0
-50
0
20
40
60
80
100
120
140
160
Time [s]

Figure 4: Comparison of surge, heave and pitch of the platform

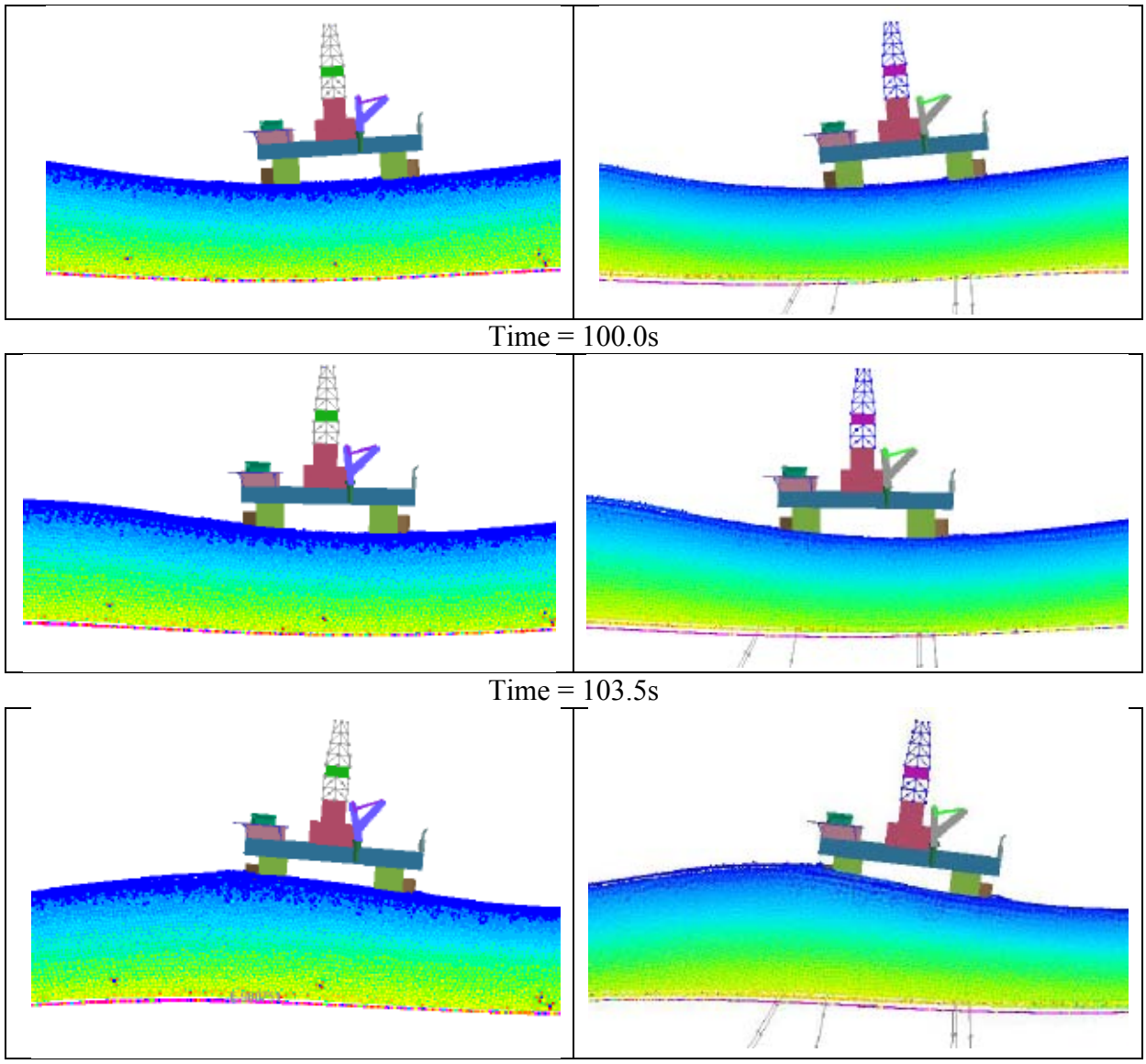

Figure 5: Interaction of the platforms with the waves

4.2 Structural Performance of Cranes

The maximum stresses in the crane structure occur at the base of the crane boom where it attaches to the tower. These stresses are caused by cantilevered bending of the boom under the influence of the motion of the platform. Figure 6 shows a top view of one crane structure, with the maximum deflections super-imposed on the undeformed crane structure. The undeformed crane is shown in black and the deformed structure in blue. In Figure 6, the image has been generated in the inertial frame of the offshore platform and hence only the displacement of the crane relative to the motion of the platform is shown.

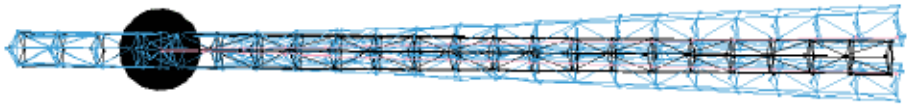

Figure 6: Deformation of crane structure under platform motion

Figure 7 shows the time histories of axial stresses induced in the truss members at the base of the crane boom. Only the histories of the four most highly stressed members are presented. Although the analyses ran for a total of 240s, only data for 2 wave periods is presented. The dashed blue line represents the raw data extracted from the analysis and the solid black line is after a 25 point moving average filter is applied to smooth the data. These time histories reveal that the truss members are subjected to cyclic stresses, often with a mean-value offset from zero. This information is important in assessing the fatigue life of the crane structure.

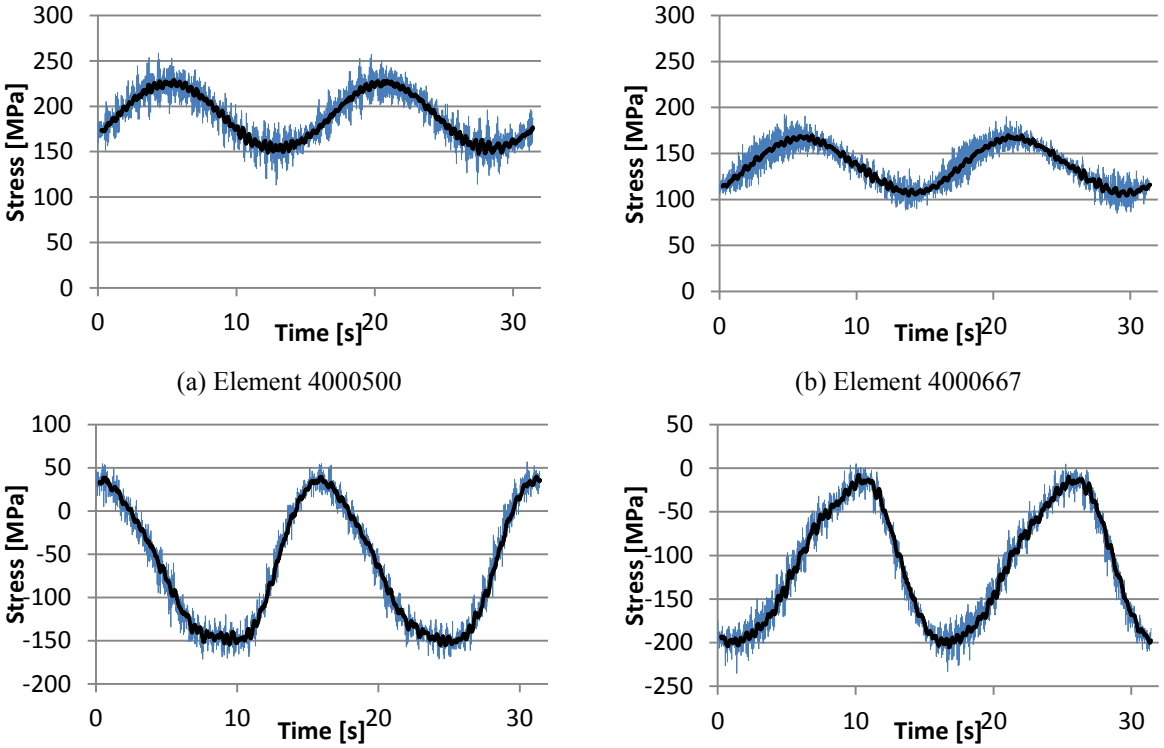

(a) Element 4000500

(b) Element 4000667

(c) Element 4000522

(d) Element 4000544

Figure 7: Axial stress time histories in crane structure

Figure 8 shows the forces transmitted through the tied interfaces at the base of the crane tower. Only two force time histories are presented in Figure 8 representing the tied interfaces

with the maximum tensile and compressive forces, respectively. These forces are an indication of the loads that must be carried by the bolts connecting the crane to the main platform structure. The forces are cyclical in nature and they have a mean-value offset from zero, either in tension or compression depending on whether the tied interface is outboard or inboard relative to the crane boom. This information is important in determining details of the bolted connections attaching the crane to the main platform structure.

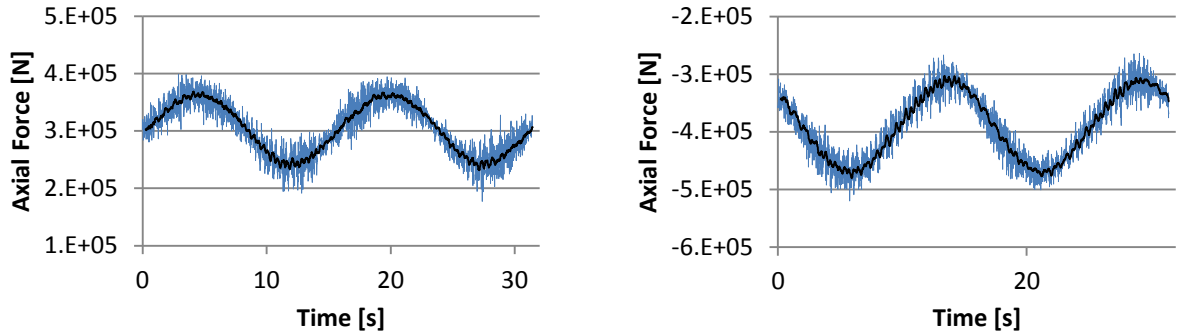

(a) Maximum tensile force (b) Maximum compressive force

Figure 8: Forces transmitted through crane attachment points

4.3 Performance Enhancement Seen with the MMC Technique

All the analyses with flexible components are run with, and without, MMC. For analyses where no MMC is used, the entire model is run on 6 CPUs using Shared Memory Parallel (SMP). For analyses where MMC is used, the main model is run on 6 CPUs using SMP while the model containing only the flexible structure is simulated on a single CPU.

Analysis Model	Time Step SPH [s]	Time Step FE [s]	Elapsed Time no MMC [hrs]	Elapsed time with MMC [hrs]
1	4.2E-03	-	162	-
2	4.2E-03	2.4E-03	286	164
3	4.2E-03	1.5E-04	4660	169

Table 2 : Summary of analysis models

Table 2 summarises the stable time steps and total elapsed (wall-clock) time for each analysis model. It shows the significant performance gain achievable, most notably a reduction in time of over 25 when MMC is used in model 3 containing both flexible anchor cables and flexible cranes. The total elapsed time for Model 3 without MMC was extrapolated after 4 weeks of execution based on the percentage completed until then.

5 CONCLUSIONS

A fully coupled FE-SPH simulation of a semi-submersible offshore platform subjected to strong wave action has been presented, in particular highlighting the exploitation of the explicit FE modules within ESI Group's VPS software tool for some structural components.

The influence of a flexible mooring system on the dynamic response of the platform has been investigated. Compared to an unmoored platform, the flexible anchor cables cause a moderate increase in the pitch and heave of the platform and a significant increase in the surge of the platform. The fluctuating stresses induced in the structural members of the cranes have been calculated along with the forces transmitted through the crane mounting points. This type of data can aid in the design of on-board equipment to ensure that it is able to withstand in-service loads.

Using MMC, the elapsed time required to simulate the motion of the offshore platform, including flexible anchor cables and flexible cranes, is reduced by a factor of over 25.

ACKNOWLEDGEMENTS

The authors would like to thank Mr Damian McGuckin of Pacific ESI for his ongoing support of this research.

REFERENCES

[1] Groenenboom P H L, Cartwright B K, "Interaction between structures and waves using the coupled FE-SPH method", *International Conference on Computational Methods in Marine Engineering, MARINE 2007*, P. Bergan , J. García, E. Oñate, and T. Kvamsdal, (Eds), © CIMNE, Barcelona, 2007.

[2] *Virtual Performance Solution 2010 Solver Notes Manual,* ESI Group, Paris, France, April 2010.

[3] Cartwright B, Xia J, Cannon S, McGuckin D, Groenenboom P, "Motion Prediction of Ships and Yachts by Smoothed Particle Hydrodynamics", In *Proceedings of the 2nd High Performance Yacht Design Conference*, Auckland 2006.

[4] Clauss, G F, "Task Related Rogue Waves Embedded in Extreme Seas", In *Proceedings of the 21st International Conference on Offshore Mechanics and Arctic Engineering*, February 2002, Oslo, Norway.

[5] Iwanowski B, Gladse R, Lefranc M, "Wave-in-Deck load on a Jacket Platform, CFD-Derived Pressures and Non-linear Structural Response", OMAE 2009

[6] Fontaine E, "On the Use of Smoothed Particle Hydrodynamics to Model Extreme Waves and their Interaction with a Structure", *Ifremer and IRCN workshop on "Rogue waves"*, Nov 2000, Brest, France.

[7] Cleary P W, Rudman M, "Extreme Wave Interaction with a Floating Oil Rig: Prediction using SPH", *Progress in Computational Fluid Dynamics*, **9**, 332-344 (2009)

[8] Cartwright B, Groenenboom P H L, McGuckin D, "A Novel Approach to Predict Non-Steady Loads on Vessels in Severe Seas", In *Proceedings of the 14th International Offshore and Polar Engineering* Conference, Toulon, France, May 23-38 2004

[9] Groenenboom P H L, Cartwright B K, "SPH Simulations of Free Surface Waves and the Interaction with Objects", In *Proceedings of ECCOMAS CFD 2010*, Jun 2010

[10] Monaghan, J.J., "Simulating free surface flows with SPH", *Journal of Computational Physics*, **110**, 399-406 (1994)

[11] Monaghan, J.J., "Smoothed Particle Hydrodynamics", *Annual Review of Astronomy and Astrophysics*, **30**, 543–574 (1992)

[12] Colagrossi, A. and Landrini, M., "Numerical simulation of interfacial flows by smoothed particle hydrodynamics", *Journal of Computational Physics*, **191**, 448-475 (2003)
[13] Meywerk, M., Decker, F. and Cordes, J., "Fluid-structure interaction in crash simulation", *Proceedings of the Institute of Mechanical Engineers*, **214**, 669-673 (1999)
[14] Haack, C., "On the use of a Particle Method for Analysis of Fluid-structure Interaction". *Sulzer Innotech Report STR_TB2000_014*, June, 2000.
[15] Climent, H., Benitez, L., Rosich, F., Rueda, F. and Pentecote, N., "Aircraft Ditching Numerical Simulation", In *Proceedings of the 25th International Congress of the Aeronautical Sciences*, Hamburg, Germany, 2006.
[16] Greve, L., Vlachoutsis, S., "Multi-scale and multi-model methods for efficient crash simulation", *International Journal of Crashworthiness*, **12**, 437-448 (2007)